

SMALL-SCALE STRUCTURE AT HIGH REDSHIFT. I. GLIMPSES OF THE INTERSTELLAR MEDIUM AT REDSHIFT ~ 3.5 ¹

MICHAEL RAUCH,^{2,3,4} WALLACE L. W. SARGENT,² AND TOM A. BARLOW²

Received 1998 September 8; accepted 1998 December 1

ABSTRACT

We obtained Keck High Resolution Echelle Spectrometer (FWHM = 4.4 km s⁻¹) spectra of images A and C of the gravitationally lensed quasar Q1422+231 ($z_{\text{em}} = 3.628$). The images are separated by 1''.3 on the sky. In an absorption system at $z_{\text{abs}} = 3.538$, gas column density variations by an order of magnitude and velocity shear on the order of 10 km s⁻¹ are observed in the low-ionization (Si II and C II) lines. The transverse separation in the absorbing cloud is estimated to be as small as 26 h_{50}^{-1} pc, corresponding to an effective angular resolution of 4 mas as seen from the Earth. In contrast, the high-ionization (C IV) gas appears mostly featureless and thus must be considerably more extended. The abundances of the elements carbon, silicon, and oxygen appear to be close to the solar values. The observation provides the first spatially and kinematically resolved probe of the interstellar medium at high redshift on scales small enough to be influenced by individual stars or star clusters. The mass associated with the low-ionization “cloudlets” is likely to be less than about 3000 M_{\odot} and possibly less than 1 M_{\odot} . The velocity shear that is seen across the lines of sight is too large to be caused by galactic bulk motion, so the velocity field of the low-ionization gas must be strongly influenced by small-scale local gasdynamics. While presently it cannot be excluded that the disturbances of the gas are due to high-velocity outflows from the background quasar, the observed velocity and density structure of the $z = 3.538$ absorption is consistent with our line of sight running through an expanding shell of gas, possibly a supernova bubble or a stellar wind.

Subject headings: galaxies: abundances — galaxies: ISM — quasars: absorption lines — quasars: individual (Q1422+231)

1. INTRODUCTION

Observations of intervening absorption in multiple, gravitationally lensed quasar (QSO) images (see, e.g., Young et al. 1981; Weymann & Foltz 1983; Foltz, Weymann, & Roeser 1984; Smette et al. 1992, 1995; Bechtold & Yee 1995; Zuo et al. 1997; Michalitsianos et al. 1997; Rauch 1998; Petry, Impey, & Foltz 1998; Lopez et al. 1999) provide a very useful tool for investigating the distribution of matter at high redshift. For example, the typical sizes of various types of high-redshift cosmic structures can be measured in a statistical sense from the numbers of coincident and anticoincident absorption systems in two separate lines of sight (LOSs); depending on the amount of spectroscopic detail available, additional inferences can be drawn about the baryonic density and velocity fields and their spatial variations. Lensing by an intervening galaxy enlarges—like a magnifying glass—any structures on spatial scales from virtually zero extent (down to the size of the QSO continuum emission region) up to the maximum beam separation (tens of kiloparsecs, at the redshift position of the lensing galaxy) by opening the projected angle between the separate QSO images to a few arcseconds, where they can be spatially resolved with ground-based telescopes.

Unfortunately, gravitationally lensed images of a given object tend to have very different brightnesses between each

other. Accordingly, the observation of at least two images that were sufficiently bright to be observed while simultaneously resolving the absorption lines had to wait for the light-gathering power of the new generation of large optical telescopes (Rauch 1998; Rauch, Sargent, & Barlow 1999).

In the first of a series of papers on the small-scale properties of high-redshift ($z \sim 3$) structures, we report here on spectra obtained with the High Resolution Echelle Spectrometer (Vogt et al. 1994) at the Keck I telescope. The A ($V = 16.7$) and C ($V = 17.3$) images of the QSO 1422+231 ($z_{\text{em}} = 3.628$; Patnaik et al. 1992) have been observed during three runs in the spring of 1998, with total exposure times of 19,600 (33,200) s for the A image (C image). Since the angular separation between the images is only about 1''.3, only spectra obtained when the seeing was less than $\sim 0''.6$ were included, a condition that was satisfied at the end of a few nights when the seeing sometimes dropped below 0''.5. A $7'' \times 0''.574$ -wide decker (giving a spectral resolution of FWHM = 4.4 km s⁻¹) was placed separately on each image, with the position angle set so as to minimize contamination from the other images. When the seeing threatened to deteriorate, the slit was shifted slightly off the center of an image and away from the other images. We estimate that the contamination of our exposures of the A and C images, by each other, are at most a few percent. The absence of significant contamination can also be judged from the fact that strong differences are observed between the LOSs in the appearance of some absorption systems.

The redshift of the lens is believed to be $z_l = 0.338$ (see Kundić, Hogg, & Blandford 1997 and Tonry 1998). Combined with the small angular splitting, this low redshift leads to transverse beam separations of less than 100 pc as far as 10 Mpc or more away from the QSO where any intervening

¹ The observations were made at the W. M. Keck Observatory, which is operated as a scientific partnership between the California Institute of Technology and the University of California; it was made possible by the generous support of the W. M. Keck Foundation.

² Astronomy Department, California Institute of Technology, Pasadena, CA 91125.

³ Hubble Fellow.

⁴ Current address: European Southern Observatory, Karl-Schwarzschild-Strasse 2, Garching, D-85748, Germany.

matter is less likely to be dynamically influenced by the quasar.

2. THE $z = 3.538$ METAL ABSORPTION SYSTEM

2.1. Description

Most of the absorption lines in the spectra of the A and C images look very similar because of their small separation (see also Bechtold & Yee 1995; Petry et al. 1998; Rauch 1998). However, striking differences are found in the appearances of some low-ionization metal absorption systems. In particular, a strong system at $z = 3.538$ for which both low- (O I, Si II, and C II) and high- (C IV and Si IV) ionization lines can be observed appears to hold clues as to the small-scale properties of the absorbing gas clouds (Fig. 1). The origin of the (proper) velocity scale in the figure has been arbitrarily set to coincide with redshift $z = 3.53792$. The beam separation here is only $\Delta r \approx 26 h_{50}^{-1}$ pc, corresponding to an effective angular resolution of 3.8 mas (for $q_0 = 0.5$). The system is blueshifted with respect to the QSO's (C IV) emission line by about 6000 km s^{-1} in the rest frame of the QSO. The actual velocity difference is

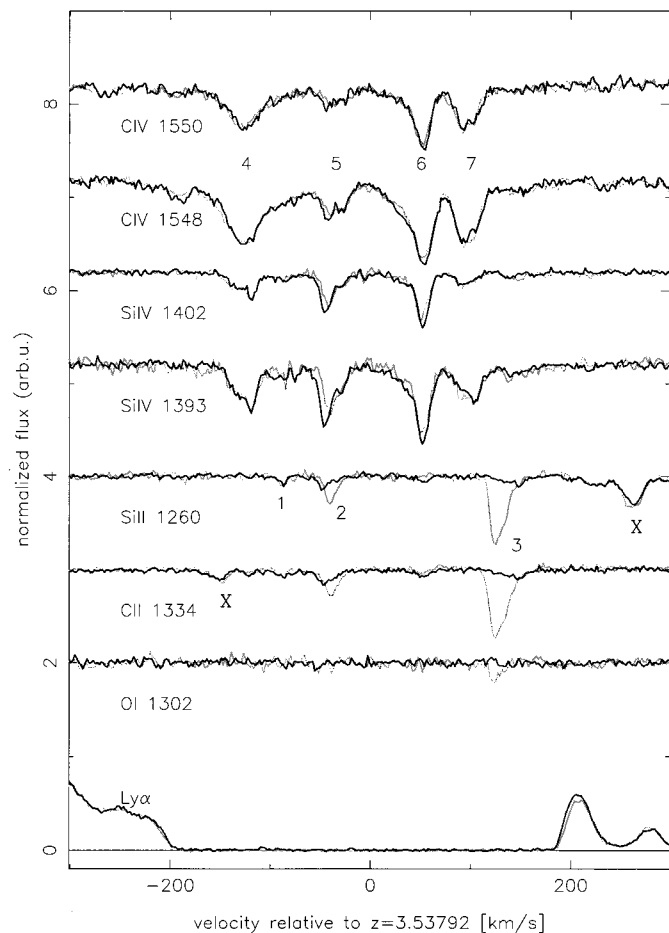


FIG. 1.—The absorption system at $z = 3.538$ as seen in the A (thin gray line) and C (thick solid line) images of QSO 1422 + 231. The plot shows the continuum-normalized flux in various ions vs. a relative velocity along the LOS (arbitrary zero point), for eight transitions. The sections are offset in the y -coordinate by suitable amounts for clarity. For convenience, some components discussed in the text are singled out by numbers. The right-most absorption line (“X” near 260 km s^{-1}) in the Si II $\lambda 1260$ region is an accidental C IV $\lambda 1548$ interloper (at $z \sim 2.7$), unrelated to the system. The X-component in the C II section of the spectrum is a similar, weak stray C IV at $z = 2.91$ (A. Boksenberg 1998, private communication).

likely to be even somewhat larger because of the blueshift commonly observed between broad and narrow (“systemic”) emission lines (Espey 1993 and references therein). It is not a priori clear whether the absorbing gas clouds are being ejected from the QSO (in which case all or a part of the redshift difference would be due to the velocity and the gas could be very close to the QSO) or whether they belong to a separate galaxy, a question we will discuss below. If independent from the QSO, the absorbing clouds are at a proper luminosity distance of $11.6 h_{50}^{-1}$ Mpc from the QSO, if we adopt $z_{\text{em}} = 3.628$ as the emission redshift, which is consistent with an origin in an intervening galaxy unrelated to the QSO.

Figure 1 shows the absorption complex as it appears (going from top to bottom) in the C IV doublet, Si IV doublet, Si II, C II, O I, and Ly α . In each case, the solid line is the spectrum of the C image, and the gray line that of the A image. For further reference, we have numbered the strongest low-ionization (1–3) and high-ionization (4–7) components.

For this particular system, the high- and low-ionization lines exhibit very different component structures. While the total velocity extent is similar ($\sim 300 \text{ km s}^{-1}$) in both cases, only component 2 appears to be clearly present in all ions. It is further interesting to note that the C IV components in the two images seem to be identical within the errors. This lack of structure indicates that the typical gas cloud giving rise to C IV lines is larger than a few tens of parsecs. From more widely separated lines of sight (Rauch 1998; Rauch, Sargent, & Barlow 1998), we also know that the structures producing individual C IV lines differ in column density by 50% or more over a few hundred parsecs to a kiloparsec, so this range appears to be characteristic of the typical sizes of C IV “cloudlets.” The Si IV absorption patterns are also very similar between the two LOS, except for some slight but significant differences in the column density and/or velocity structure of component 2. The observed differences can be interpreted as a shift in column density-weighted velocity by $\Delta v = v_A - v_C \approx 3 \text{ km s}^{-1}$ between the two lines of sight. A similar shift is also visible in Si II $\lambda 1260$ and C II $\lambda 1334$ ($\Delta v \approx 5 \text{ km s}^{-1}$ for component 2; $\Delta v \approx -16 \text{ km s}^{-1}$ for component 3). However, the most striking difference is found between the low-ionization column densities across the LOS (see Table 1). Component 2 has a Si II (C II) column 2.1 (2.4) times larger in the A image; the strongest low-ionization component 3 is even 10.5 (10.0) times stronger in the A than in the C image.

2.2. Physical State and Mass⁵

Constraints on the ionization parameter, metallicity, and density of the absorbing gas can be obtained by using observations of several ions (see, e.g., Bergeron & Stasinska 1986; Chaffee et al. 1986; Steidel 1990; Donahue & Shull 1991). First, we note that system 3 is apparently optically thin to ionizing radiation, which is somewhat surprising given the strength of the low-ionization lines Si II and C II. From a direct Voigt profile fit to several lines of the Lyman series (up to Lyman 7), we get $\log N(\text{H I}) = 16.05 \pm 0.15$ (with N measured in units of cm^{-2}) for component 3, in LOS A; the error gives only the uncertainty of the fit. For

⁵ Unless other components are mentioned explicitly, the analysis below will be focused on the strongest low-ionization component (component 3) in the A image.

TABLE 1
LOG: COLUMN DENSITIES OF VARIOUS LOW-IONIZATION LINES

LOS	COMPONENT 1		COMPONENT 2		COMPONENT 3	
	A	C	A	C	A	C
Si II	11.53 ± 0.11	11.37 ± 0.08	12.13 ± 0.03	11.81 ± 0.04	12.82 ± 0.01	11.80 ± 0.05
C II	12.05 ± 0.12	12.18 ± 0.14	13.14 ± 0.03	12.76 ± 0.04	13.73 ± 0.01	12.73 ± 0.06
O I	<12.7	<12.7	<12.7	<12.7	13.27 ± 0.06	<13.0
Si IV	12.77 ± 0.05	12.85 ± 0.06	<12.0	<12.0
C II/Si II	0.52 ± 0.16	0.81 ± 0.16	1.01 ± 0.04	0.95 ± 0.06	0.91 ± 0.01	0.93 ± 0.08

most of the Lyman series except Ly α , there may be systematic uncertainties in both the continuum and the zero-level placement, and the systematic error may be considerably larger than that quoted above. Unfortunately, the spectra are quite noisy in the blue, and they do not cover the Lyman limit of the system. Thus, the H I column density is not very precisely known, although trials (assuming the same Doppler parameter $b = 21 \text{ km s}^{-1}$) show that a column density of $\log N = 16.5$ is clearly too high. Accordingly, unless the Doppler parameter is much smaller and the line is unresolved even at our resolution, the aforementioned value is a conservative upper limit. [The system in question has been detected in earlier observations of Q1422 + 231 by ourselves and independently by Songaila & Cowie 1996, who find a total H I column density $N(\text{H I}) = 2.3 \times 10^{16} \text{ cm}^{-2}$. However, these older spectra were not taken for the purpose of splitting the contributions from separate images.] A comparison of the absorption-line strength between low- and high-ionization species shows immediately that the gas of component 3 must be of rather low ionization. We have used the results of the photoionization calculations of Donahue & Shull (1991, hereafter DS) summarized in their Figure 7 (they used a typical QSO spectrum after Matthews & Ferland 1987 and a metallicity $Z = 0.1 Z_{\odot}$, assuming solar relative abundances). Our observed column density ratios of neutral oxygen to singly ionized carbon,

$$\log \frac{N(\text{O I})}{N(\text{C II})} = -0.45 \pm 0.06, \quad (1)$$

imply an ionization parameter

$$\log U = \frac{n_{\gamma}}{n} \simeq -4.4, \quad (2)$$

in agreement with the upper limit from the Si II/Si IV ratio,

$$\log U \leq -3.4. \quad (3)$$

The total H density n , again according to DS, is then

$$n \simeq 1.6 \left(\frac{J_{912}}{10^{-21}} \right) \text{ cm}^{-3} \quad \text{and} \quad n \geq 0.16 \left(\frac{J_{912}}{10^{-21}} \right) \text{ cm}^{-3}, \quad (4)$$

respectively, for the two U -values, where J_{912} is the intensity of the radiation field at the Lyman limit averaged over $4\pi \text{ sr}$, in units of $\text{ergs cm}^{-2} \text{ Hz}^{-1} \text{ s}^{-1} \text{ sr}^{-1}$.

In spite of its low H I column density, the neutral fraction of the gas must be as large as 0.15 (0.014) for $\log U = -4.4$ (-3.4). For $J = 10^{-21} \text{ ergs cm}^{-2} \text{ s}^{-1} \text{ Hz}^{-1} \text{ sr}^{-1}$, and using the inferred H density, H I column density, and neutral fraction, we get a size estimate along the line of sight,

$$L \sim 0.015 \text{ pc and } L \leq 1.6 \text{ pc}. \quad (5)$$

It is important to bear in mind that these derivations are assuming thermal photoionization equilibrium with a QSO radiation field, which may not be very realistic.

An independent upper limit on the density can be obtained from the absence of the ($J = 1/2 \rightarrow 3/2$) fine-structure transitions in C II* $\lambda 1335.7$ and Si II* $\lambda 1264.7$ (Bahcall & Wolf 1968; York & Kinahan 1979). Here C II* gives a somewhat tighter upper limit than Si II*. We observe

$$\frac{N(\text{C II}^* \lambda 1335.7)}{N(\text{C II} \lambda 1334.5)} \leq 0.04, \quad (6)$$

from which we get an approximate upper limit on the electron density of

$$n_e \leq 1.5 \times \left(\frac{T}{10^4 \text{ K}} \right)^{0.5} \text{ cm}^{-3} \quad (7)$$

(valid for temperatures above a few hundred kelvins). Assuming that most of the gas is ionized, $n \simeq n_e$, an upper limit close to the maximum density allowed by the DS photoionization models is obtained, implying that the density must be somewhere in the range

$$0.16 \leq n \leq 1.6 \text{ cm}^{-3}. \quad (8)$$

We know that the transverse size of the clouds (i.e., the distance over which the column density decreases by a factor of 10) is on the order of 26 pc. The gas mass associated with the cloud can then be estimated very crudely to lie between that of a homogeneous, cylindrical slab of size $L\pi(\Delta r)^2$ (assuming the smallest value for L and a radius Δr), on one hand, and (ignoring the photoionization size estimates) a spherical cloud with a radius Δr and the high-density limit, on the other:

$$0.4 \leq M \leq 2700 M_{\odot}. \quad (9)$$

The assumption of homogeneity is of course questionable. In any case, the scale indicates that, for the first time, we are resolving structure on scales relevant to individual star clusters or even single stars in a high-redshift galaxy.

The remaining absorption components visible in C II and Si II appear to have less extreme ionization states. Component 2 appears in all ions except O I. The ionization parameter (in LOS A) is measured to be

$$\log U \simeq -2.7 \text{ (from Si II/Si IV)}$$

and

$$\log U \simeq -2.8 \text{ (from C II/C IV)}, \quad (10)$$

typical for stronger high-ionization systems when both Si IV and C IV are detected. In deriving U , it is assumed that the singly ionized and triply ionized gas clouds have the same spatial extent. In general, this is not true, as can be seen directly from the larger sizes inferred for most C IV systems. However, for this particular component, both the C IV and the Si IV seem to trace the shift in the velocity between the LOSs seen in the low ions reasonably well, so most of the C IV here may indeed occupy a similar volume as the C II.

The other high-ionization components 4, 6, and 7 are unexceptional in that there are hardly any column density or velocity differences between the LOSs, and the ionization level is consistent with the observed range of C IV systems. For example, for component 6, $\log U \simeq -2.5$. This is in spite of the relative proximity of the QSO; one would expect a higher degree of ionization if the QSO's radiation field dominates over the metagalactic background. We have tried to detect N V absorption, a characteristic sign of gas associated with the large ionizing intensity near the QSO, at the positions of the known C IV components, weighted by the model C IV column density ratios. Only an upper limit of $\log N(\text{N V}) < 12.25$ (1σ) for the total N V column of the $z = 3.538$ system was found. Compared with the total C IV column $\log N(\text{C IV}) = 14.34 \pm 0.03$, this leads to an upper limit on the averaged ionization parameter $\log U < -3.2$. This is somewhat less than the U -values measured for the individual high-ionization components from other ion ratios (see above), and it may imply that either the nitrogen abundance is lower than solar relative to C or Si, or that there is a lack of high-energy photons capable of ionizing N IV, as is indeed expected for a radiation field dominated by starlight.

2.3. Temperatures

In the case of the high-ionization component 4, the absorption line can be modeled as three relatively broad components. Even the apparently narrow "Gaussian core" of the line requires a component with $b = 14 \text{ km s}^{-1}$, corresponding to a temperature of greater than $1.5 \times 10^5 \text{ K}$, if thermal. This b -value is considerably larger than the typical thermal width of C IV lines ($b_{\text{median}} \sim 7 \text{ km s}^{-1}$, corresponding to $T \sim 4 \times 10^4 \text{ K}$; Rauch et al. 1996). The broad wings are not repeated in the Si IV profile, perhaps implying that additional hot (collisionally ionized) gas contributes to the C IV profile. However, cooler gas is present as well. Lines 6 and 7, while also containing asymmetric broad wings, do have cores more similar to typical C IV widths: line 6 has a dominant component with $b = 8.9 \text{ km s}^{-1}$, and line 7 has one with $b = 6.4 \text{ km s}^{-1}$; both lines are consistent with mostly thermal broadening caused by photoionization.

The low ions clearly show lower temperatures. Returning to component 3, the line appears to be a blend of several components, which can be modeled as three Voigt profiles. The sharp blue wing of C II (Si II) is well fitted by $b_{\text{C II}} =$

$4.10 \pm 0.50 \text{ km s}^{-1}$ ($b_{\text{Si II}} = 3.95 \pm 0.33 \text{ km s}^{-1}$). The similarity of the values indicates that bulk motion is more important than thermal broadening. Thus, we have an upper limit to the temperature, $T < 1.2 \times 10^4 \text{ K}$.

2.4. Metallicities

The metal abundance of at least one component of the system appears to be rather high. Using the measured O I/C II ratio of component 3, together with the relations between the ion abundance and the U -parameter from DS, we predict $\log [N(\text{O I})/N(\text{H I})] \simeq -4.0$, whereas, from the measured $N(\text{H I})$, we would expect $\log [N(\text{O I})/N(\text{H I})] \simeq -2.8$. Similarly, the predicted $\log [N(\text{Si II})/N(\text{H I})] \leq -4.2$, in contrast to the measured -3.2 . The DS model was for a metallicity $Z = 0.1 Z_{\odot}$, so raising the abundances to approximately solar gives consistent values. The relative abundances appear to be close to solar as well. Assuming that the ionization parameter $\log U = -4.4$ (derived from the O I/C II ratio) holds, the C II/Si II ratio is expected to be $\log [N(\text{C II})/N(\text{Si II})] \simeq 1.1$, which is not very different from any of the observed values for $\log [N(\text{C II})/N(\text{Si II})]$ given in Table 1. Even if the O/C would be higher than solar (as in metal-poor stars) so that the true ionization parameter would be higher than estimated here, the conclusion that Si/C is solar would still hold, since C II/Si II is rather insensitive to the ionization parameter.

3. POSSIBLE INTERPRETATIONS: EJECTED GAS OR INTERVENING GALAXY?

Given the relative proximity of the system to the QSO, one may wonder whether the gas is possibly ejected from the QSO host galaxy and, therefore, classified among the so-called $z_{\text{abs}} \simeq z_{\text{em}}$ systems. The main properties of these systems are as follows: absorption redshift close to or beyond the emission redshift of the QSO; only partial coverage of the QSO's emission region; high (supersolar) metallicity; and a high-ionization state caused by the active galactic nucleus radiation field, which is evident, for example, through the presence of N V. Petitjean, Rauch, & Carswell (1994) have found high-metallicity systems out to $13,000 \text{ km s}^{-1}$ from the QSO emission redshift, and with a velocity separation of $\sim 6000 \text{ km s}^{-1}$, the $z = 3.538$ system is within that range. However, the H I lines corresponding to components 2 and 3 do go down to zero intensity, so the clouds must be covering the QSO continuum and line-emitting regions completely. Moreover, we do not find N V in any of the components down to limits lower than any of the individual N V upper limits or detections in the Petitjean et al. data, nor do we detect (see above) high [Si/C] ratios as did Savaglio, D'Odorico, & Møller (1994) in their $z_{\text{abs}} \simeq z_{\text{em}}$ sample. Models of galactic chemical evolution (Matteucci & Padovani 1993) show that the presently observed abundance pattern (C, Si solar, $N \leq$ solar), unlike the pattern seen in many QSO emission-line spectra and many $z_{\text{abs}} \simeq z_{\text{em}}$ systems (N, Si enhanced by up to an order of magnitude, C and O solar), can be produced in the very early phases of galactic nucleosynthesis, shortly after the onset of the first starburst in an elliptical galaxy (t less than a few times 10^8 yr), even before the QSO abundance anomalies (see, e.g., Hamann 1997) are established. Nevertheless, it cannot be excluded that the system is ejected or at least dynamically influenced by the QSO. Radiation pressure or ram pressure from outflows may explain why the lower density, high-ionization gas seems to be blueshifted with

respect to the denser low-ionization clumps, from which the C IV gas may have been ablated like a cometary tail.

If, however, the absorption system is not influenced dynamically by the QSO, where do the small-scale velocity variations across the LOS come from? On a scale of 26 pc, the velocity shear observed most prominently in components 2 and 3 (about 10 km s^{-1}) is on the order of $\Delta v_{\parallel}/\Delta r \sim 400 \text{ km s}^{-1} \text{ kpc}^{-1}$ (across the sky and projected along the LOS). This is too large to be caused by rotation on a galactic scale. Therefore, we must look to local gas-dynamics for an explanation of the observed motions. It turns out that an expanding shell of gas gives a consistent explanation for the observed velocity and column density pattern (Fig. 2): closer inspection shows that the components 2 and 3 are weaker in the C spectrum; they are also more widely spaced than in A, and they exhibit asymmetric tails pointing toward each other. Figure 2 shows (in a schematic drawing) how this pattern can arise if we are looking along two LOSs intersecting an expanding spherical shell, where one of the LOSs intersects the expanding gas more peripherally than the other. The velocity shear projected along the LOS is caused by the projected expansion velocity, $\Delta v_A = 2v_{\text{exp}} \cos \theta_A$ being smaller than Δv_C on account of the more tangential contact of LOS A. The longer path length of LOS A through the shell also may account for the higher column density of the absorption lines in A. The fact that there is a noticeable velocity difference means that the radius of the shell (always presuming a spherical homogeneous geometry) is indeed not much larger than the transverse beam separation $\Delta r = 26 \text{ pc}$. For a spherical shell, the radius R is linked to the impact parameters of the LOS from the center of the shell, b_A and b_C , the beam separation $\Delta r (= b_C - b_A)$, and the observed velocity separations between the two absorption lines that are supposed to be caused by the expanding shell (components 2 and 3) Δv_A and Δv_C by

$$R^2 = \frac{(b_C + \Delta r)^2 - b_C(\Delta v_A/\Delta v_C)^2}{1 - (\Delta v_A/\Delta v_C)^2}, \quad (11)$$

where $\Delta v_A/\Delta v_C = 0.84$ (the velocity separations are measured between the peaks of the components 2 and 3). Since

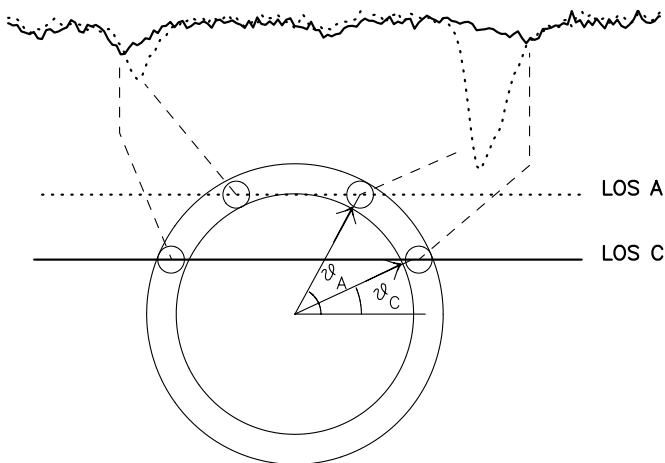


FIG. 2.—A speculative schematic diagram showing how the low-ionization absorption pattern (C II $\lambda 1334$ region) may arise when LOS A (dotted line) and C (solid line) intersect an expanding shell of gas at different impact parameters and with different angles θ_A and θ_C between the expansion velocity vector and the LOS.

b_C can vary between $b_C = 0$ and $b_C = R - \Delta r$, we find

$$13 \leq R \leq 48 \text{ pc}. \quad (12)$$

Since the absolute impact parameters of the LOS from the center of the shell are unknown, we can only get a lower limit to the velocity of expansion v_{exp} from the velocity width measured between the absorption maxima of components 3 and 4 along LOS C:

$$2v_{\text{exp}} \geq 195 \text{ km s}^{-1}. \quad (13)$$

4. DISCUSSION

We can summarize the main findings as follows: low-ionization QSO absorption systems (as defined by the presence of singly ionized Si, C, etc.) can be very small entities that change significantly over scales of tens of parsecs. This appears to be distinct from the properties of the high-ionization gas (C IV systems), the density and velocity structure of which changes only over separations exceeding a few hundred parsecs (Rauch 1998; Rauch et al. 1999). Our directly measured sizes clearly confirm long-standing predictions based largely on ionization arguments (Sargent et al. 1979; Bergeron & Stasinska 1986; Giroux, Sutherland, & Shull 1994; Petitjean, Riediger, & Rauch 1996) that the absorption indeed arises in an inhomogeneous gas with several ionization phases and a different spatial extent.

To explain the finding of velocity differences over tens of parsecs, we must conclude that low-ionization QSO absorption systems derive their internal velocity dispersion from local gasdynamics, originating either from the host galaxy of the background QSO itself or from stellar sources of momentum in an intervening galaxy. While the relatively high metallicities, together with the proximity (in velocity) to the background QSO, are consistent with the gas being associated with the QSO host galaxy, the low-ionization state, the full coverage of the QSO emission regions, and the absence of peculiar abundance patterns argue against this possibility.

It is hard to say what the precise origin of these absorption features is. We have argued here that an expanding gas shell like a bubble blown by a stellar wind or a supernova, while not being a unique explanation, is quite consistent with the data. Indeed, Shi (1995) has drawn attention to the possibility that Type II supernova shells may explain the large velocity dispersions often seen in C IV systems. Simulations of the formation of high-redshift galaxies indicate that the velocity width of typical C IV systems is more likely to reflect the velocity structure of larger, galaxy-forming regions (see, e.g., Rauch, Haehnelt, & Steinmetz 1997) than individual supernovae, but we suggest here that a supernova or stellar wind origin may well be more relevant for the denser environment of some of the low-ionization systems, possibly associated with galactic disks or the denser regions of halo clouds. As Shi (1995) points out, a “standard” Type II supernova explosion energy release (10^{51} ergs) is sufficient to accelerate $10^4 M_{\odot}$ of matter to an expansion velocity of 100 km s^{-1} , which is well consistent with the energy requirements in the present case.

Summarizing, it appears that the two-dimensional information provided by close, multiple LOSs allows us for the first time to resolve the spatial and kinematic structure of an individual low-ionization absorption system. At the same time, this observation demonstrates that with the new generation of large optical telescopes, we are now in a position

to study the interstellar medium at arbitrarily high redshift. It is likely that such observations will reveal familiar astrophysical environments like supernova shells or stellar winds. The much earlier stage in the cosmic development at $z \sim 3.5$ (for example, the influence of shallower potential wells on the gasdynamics, the onset of nucleosynthesis as a function of the density of the environment, etc.) may ultimately show up in larger data sets of this kind.

Judging from a single case, it is not possible to say whether small-scale motions, *in general*, play a role as important as suggested here, even if most of the low-ionization clumps should indeed have a local, stellar origin. But if so, the measured velocity dispersion of an absorption system, consisting of the quadratic sum of the *local* velocity dispersion (for example, $2v_{\text{exp}}$, if caused by an expanding shell) and the *galactic large-scale* motion, may receive a dominant contribution from the former. In that case, attempts at modeling the kinematics of absorption systems solely in terms of gravitational motions (e.g., as rotation of galactic disks) may be overestimating the depth of the underlying galactic potential wells.

Finally, at present, the success of a future statistical study of the high-redshift interstellar medium with this method crucially depends on more bright, high-redshift ($z > 2$)

lensed QSOs being found with at least two bright images and image separations in excess of $1''$ – $1.5''$. Unfortunately, a typical lensed QSO usually has (if at all) only one image bright enough ($V < 19$) for spectroscopy with a 10 m class telescope, and it shows image separations of less than $1.5''$ so that the majority of lensed objects are just not accessible to high-resolution observations. Thus, a promising future observational approach, providing the spatial resolution necessary to split the images and, at the same time, the needed higher signal-to-noise ratio, will probably involve adaptive optics in conjunction with an optical or infrared high-resolution spectrograph.

We thank the W. M. Keck Observatory Staff for their help with the observations and for their readiness to depart from standard observing procedures, Alec Boksenberg for correcting the identification of one of the absorption systems, Bob Carswell for useful discussions and for help with the fitting program, and Martin Haehnelt for reading an earlier draft. M. R. is grateful to NASA for support through grant HF-01075.01-94A from the Space Telescope Science Institute. W. L. W. S. and T. A. B. were supported by grant AST 95-29073 from the National Science Foundation.

REFERENCES

- Bahcall, J. N., & Wolf, R. A. 1968, *ApJ*, 152, 701
 Bechtold, J., & Yee, H. K. C. 1995, *AJ*, 110, 1984
 Bergeron, J., & Stasinska, G. 1986, *A&A*, 169, 1
 Chaffee, F. C., Foltz, C. B., Bechtold, J., & Weymann, R. J. 1986, *ApJ*, 301, 116
 Donahue, M., & Shull, M. 1991, *ApJ*, 383, 511 (DS)
 Espey, B. R. 1993, *ApJ*, 411, L59
 Foltz, C. B., Weymann, R. J., & Roeser, H.-J. 1984, *ApJ*, 281, L1
 Giroux, M. L., Sutherland, R. S., & Shull, J. M. 1994, *ApJ*, 435, L97
 Hamann, F. 1997, *ApJS*, 109, 279
 Kundić, T., Hogg, D. W., & Blandford, R. D. 1997, *AJ*, 114, 2276
 Lopez, S., Reimers, D., Rauch, M., Sargent, W. L. W., & Smette, A. 1999, *ApJ*, in press (astro-ph/9806143)
 Matteucci, F., & Padovani, P. 1993, *ApJ*, 419, 485
 Matthews, W. D., & Ferland, G. 1987, *ApJ*, 323, 456
 Michalitsianos, A. G., et al. 1997, *ApJ*, 474, 598
 Patnaik, A. R., Browne, I. W., Walsh, D., Chaffee, F. H., & Foltz, C. B. 1992, *MNRAS*, 259, 1P
 Petitjean, P., Rauch, M., & Carswell, R. F. 1994, *A&A*, 291, 29P
 Petitjean, P., Riediger, R., & Rauch, M. 1996, *A&A*, 307, 417
 Petry, C. E., Impey, C. D., & Foltz, C. B. 1998, *ApJ*, 494, 60
 Rauch, M. 1998, in *Proc. 13th IAP Colloq., Structure and Evolution of the IGM from QSO Absorption Lines*, ed. P. Petitjean & S. Charlot (Paris: Editions Frontières), 109
 Rauch, M., Haehnelt, M. G., & Steinmetz, M. 1997, *ApJ*, 481, 601
 Rauch, M., Sargent, W. L. W., & Barlow, T. A. 1998, in *ASP Conf. Ser. 146, The Young Universe: Galaxy Formation and Evolution at Intermediate and High Redshift*, ed. S. D'Odorico, A. Fontana, & E. Giallongo (San Francisco: ASP), 167
 ———. 1999, in preparation
 Rauch, M., Sargent, W. L. W., Womble, D. S., & Barlow, T. A. 1996, *ApJ*, 467, L5
 Sargent, W. L. W., Young, P. J., Boksenberg, A., Carswell, R. F., & Whelan, J. A. J. 1979, *ApJ*, 230, 68
 Savaglio, S., D'Odorico, S., & Møller, P. 1994, *A&A*, 281, 331
 Shi, X. 1995, *ApJ*, 449, 140
 Smette, A., Robertson, J. G., Shaver, P. A., Reimers, D., Wisotzki, L., & Koehler, T. 1995, *A&A*, 113, 199
 Smette, A., Surdej, J., Shaver, P. A., Foltz, C. B., Chaffee, F. H., Weymann, R. J., Williams, R. E., & Magain, P. 1992, *ApJ*, 389, 39
 Songaila, A., & Cowie, L. L. 1996, *AJ*, 112, 335
 Steidel, C. C. 1990, *ApJS*, 74, 37
 Tonry, J. L. 1998, *AJ*, 115, 1
 Vogt, S. S., et al. 1994, *Proc. SPIE*, 2198, 362
 Weymann, R. J., & Foltz, C. B. 1983, *ApJ*, 272, L1
 York, D. G., & Kinahan, B. F. 1979, *ApJ*, 228, 127
 Young, P. J., Sargent, W. L. W., Boksenberg, A., & Oke, J. B. 1981, *ApJ*, 249, 415
 Zuo, L., Beaver, E. A., Burbidge, E. M., Cohen, R. D., Junkkarinen, V. T., & Lyons, R. W. 1997, *ApJ*, 477, 568